Transactions of the Korean Nuclear Society Spring Meeting
Jeju, Korea, May 18-19, 2017

Evaluation of Thermal Aging Effect on Stress Corrosion Cracking Resistance in Fusion Boundary of A533 Gr. B and Alloy 152

Kyoung Joon Choi [a], Seung Chang Yoo [a], Taeho Kim [a], Seunghyun Kim [a] and Ji Hyun Kim [a*]
[a] *Department of Nuclear Engineering, School of Mechanical, Aerospace and Nuclear Engineering, Ulsan National Institute of Science and Technology, 50 UNIST-gil, Ulsan, 44919*
[*] *Corresponding author: kimjh@unist.ac.kr*

1. Introduction

Dissimilar metal weldment (DMW) is frequently used for joining low-alloy steel pressure vessel nozzles and steam generator nozzles to nickel-based wrought alloy or austenitic stainless steel components in high-energy systems. The thermal expansion coefficient of Ni-based weld metal lies between those of the substrates, i.e., a nickel-base wrought alloy and low-alloy steel. This feature also significantly hinders C diffusion from the ferrite base metal to the weld metal. Until now, stress corrosion cracking has not occurred in DMWs where a High-Cr weld metal (such as Alloy 152 or Alloy 690), which is Ni-base weld metal including relative high Cr, is used as the weld metal in the weld between the nickel-based alloy and low-alloy steel.

However, current operational experience is thought to be too short to justify the conclusion that High-Cr weld metals are perfectly immune to stress corrosion cracking.

Although serious cracking issues may not occur in as-welded materials, thermal aging may change the local microstructure and residual stress, affecting the cracking resistance or strength. There is not sufficient study on the effect of thermally aging on stress corrosion cracking. Among weld joints, the fusion boundary (FB) region is expected to be the most susceptible to thermal aging effects owing to the chemical gradient formed during welding.

Therefore, to investigate the resistance on stress corrosion cracking in FB region in as-welded and aged DMWs used in operating power plant systems, corrosion behavior and mechanical property were evaluated by exploiting electrochemical experiments and nano-indentation. Additionally, crack growth rate measurement for evaluating stress corrosion cracking resistance was performed with crevice bent beam test method.

2. Experimental

DMW joints of A533 Gr. B/Alloy 152/ Alloy 690 was used in this study. A representative mockup sample, consisting of A533 Gr. 3/Alloy 152/Alloy 690, was fabricated with welding process based on ASME Section IX. First, A533 Gr. B was coated with Alloy 152 weld metal, which formed three buttering layers.

Once low-alloy steel block was buttered with Alloy 152, a post-weld heat treatment was performed at 607–635 ºC for 3 h. Then heat treatment to simulate the long-term effects of thermal aging was performed through high temperature heat treatment since it takes too long to duplicate the actual thermal history in a NPP for 15 or 30 years at 320 °C. The detail method used was explained in elsewhere [1]. Specimens were produced to three different heat treatment times to simulate long-term thermal aging effects for 0, 15, and 30 years. In case of A533 Gr. B/Alloy 152/ Alloy 690, the corresponding heat treatment times and name were 0 h (As-welded), 6,450 h (HT400_Y15), and 12,911 h (HT400_Y30) at 400 °C. The corrosion behavior of the as-received and the thermally aged samples were then analyzed by potentiodynamic electropolarization using a potentiostat (Princeton Applied Research, PAR 273A, US).

Prior to experiment, the samples were immersed in solution and their open circuit potential (OCP) was measured to obtain a steady-state OCP with a potential fluctuation less than 10 mV. The solution simulating the conductivity of the primary water in the nuclear power plant, with 0.1M sodium borate (borate buffer solution) and boric acid, was prepared and purged with high-purity nitrogen gas to eliminate dissolved oxygen. For the experiments, a three-electrode system was prepared with platinized platinum-mesh as a counter electrode, a saturated calomel electrode (SCE, 0.241 VSHE vs. SHE) as a reference electrode, and the samples as the working electrode. The scan rate was set to 0.1 mV/sec.

Nanoindentation tests were performed using an Agilent Technologies Nano Indenter G200 and a continuous stiffness measurement technique, in which a three-sided pyramidal Berkovich tip was used for nanoindentation. The experimental conditions used were as follows: a total penetration depth of 1000 nm, a strain rate of 0.05 s^{-1}, and a Poisson's ratio of 0.3. In each specimen, all of 15 indentation points were measured along the FB region.

In the hardness-displacement curve, hardness was achieved by averaging the indentation hardness at a displacement from 700 nm to 1000 nm for each indentation. To improve the reliability of the results, the average hardness of the 15 indentation points in the FB region was calculated. Crack growth rate was measured at 25 cm^3/kg DH concentration through crevice bent beam test which was performed following the experiments described in the previous study [2]. The tests were performed in a 3.79 L stainless steel autoclave, which can maintain conditions of 1200 ppm (mg/kg) B, 2 ppm (mg/kg) Li, 25 cm^3/kg of DH concentration, dissolved oxygen < 5 ppb, 325 °C, and 15 MPa. Proper amount of boric acid (H_3BO_3) and lithium hydroxide monohydrate (LiOH) were added in dilated water to simulate the primary coolant of nuclear power plant and electronic conductivity of this solution were maintain to 21~22 μS/cm. Then DH was controlled by overpressure with 99 % hydrogen gas.

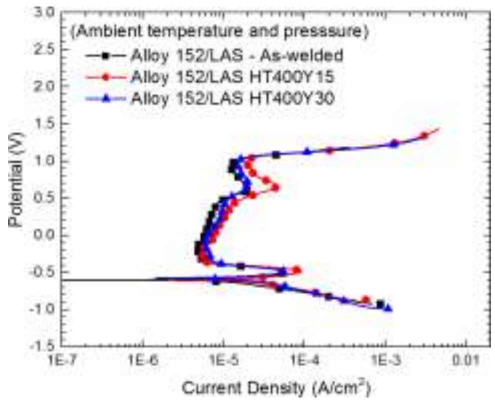

Fig. 1 Potentiodynamic polarization curves at the interface between low-alloy steel and Alloy 152

Table 1 Corrosion resistance and current density calculated with the polarization curves in Fig. 1

Specimen	LAS/Alloy152			
	B_{anode}	B_{cahode}	I_0(μA/cm^2)	V_0(V)
As-welded	742.5	486.8	9.49	-0.653
HT400Y15	859.9	693.0	12.02	-0.630
HT400Y30	511.8	566.4	9.15	-0.658

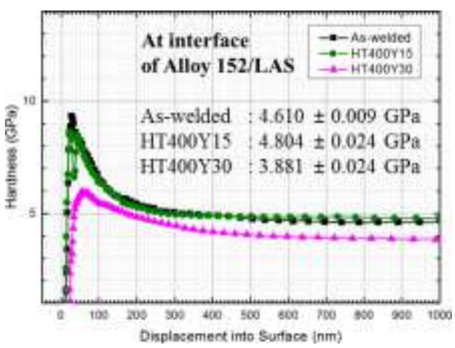

Fig. 2 Hardness-displacement into surface of the fusion boundary region between low-alloy steel and Alloy 152

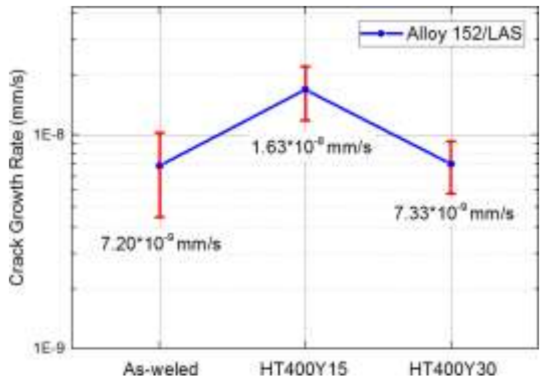

Fig. 3 Crack growth rates, measured though crevice bent beam test, of the fusion boundary region between low-alloy steel and Alloy 152

3. Results and Discussion

To evaluate the thermal aging effects on corrosion behavior at the interface, FB, between low-alloy and Ni-base weld metal. two DMW joints of A533 Gr. B/Alloy 152/ Alloy 690 were used for potentiodynamic polarization experiments and Nano-indentation test.

The potentiodynamic polarization curves, shown in Fig. 2, represent the corrosion characteristics of FB regions: low-alloy steel/Alloy 152. The test data was summarized in Table 1.

Once, in the result of FB region of low-alloy steel and alloy 152, the corrosion rate (exchange current density or Tafel slopes shown in Table 1) increased with thermal aging heat treatment, representing that the corrosion rate increased after heat treatment time equivalent to 15-yr, but re-decrease after one to 30-yr (as shown in Table 1).

It seems that the corrosion resistance was affected from the changes of the Cr rich precipitate's morphology and residual stress by thermal aging. In corrosion, Cr-rich precipitates play an important role in the mechanical response of steel since there act as hard particle, cause pitting corrosion and degradation of passivity. Residual stress, which formed in the FB region by buttering welding process and phase change during welding, can affect corrosion resistance by changing surface activity.

The hardness values as a function of penetration depth are shown in Fig. 2. The hardness values were found for penetration depths at which the hardness was maintained or did not change with penetration depth. The hardness values were measured in the range of penetration depths from 700 nm to 1,000 nm. Based on the results, the hardness values of as-welded, HT400-Y15, HT400-Y30 were 4.610 ± 0.009 GPa, 4.804 ± 0.024 GPa and 3.881 ± 0.024 GPa. It was acknowledged that the hardness was affected from the changes of the Cr rich precipitate's morphology [3-5].

Precipitates interrupt the movement of dislocation in the material and cut dislocations, resulting in hardening of the material. Dislocations cannot be cut by sufficiently grown precipitates.

In the previous study, it was observed that thermal aging causes that the number of the precipitates increases at initial step (heat treatment equivalent to 15-yr) and re-decreases by coarsening of precipitates at further step (equivalent to 30-yr) [1]. Next, thermal aging heat treatment can relax the compressive residual stress by inducing the thermal creep.

In that, at initial step, an increase in number of precipitates seems to cause the increase of the corrosion rate and hardness and the reduction of passivity in FB region of low-alloy steel and Alloy 152.

However, at further step, a decrease in number of the precipitates re-decreases the corrosion rate and hardness although the corrosion rate is higher than as-welded sample.

As the results, the crack growth rates of as-welded, HT400-Y15, HT400-Y30 were 7.20E-9 ± 3.07E-9 mm/s, 1.63E-8 ± 4.63E-9 mm/s and 7.33E-9 ± 2.00E-9 mm/s.

As the results, HT400Y15 seems relatively susceptible to stress corrosion cracking growth as show in Fig. 3 because of the accelerated galvanic corrosion and material hardening by additional formation of Cr rich precipitates.

4. Conclusions

To understand the microstructure and corrosion evolution on fusion boundary between low-alloy steel and Ni-base weld metal, microstructural analysis and polarization test were performed with A533 Gr. B/Alloy 152/Alloy 690. Remarkable changes were observed in mechanical properties, corrosion resistance and crack growth rate in fusion boundary region between low-alloy steel and Ni-base weld metal. The thermal aging treatment causes the formation and growth of precipitates and relaxation of residual stress.

The precipitate, which has different potential with peripheral region, can cause galvanic corrosion or pitting corrosion and is the one of hardening methods by disturbing movement of the dislocation.

At initial step of heat treatment, the number of precipitates was increased. In fusion boundary between A533 Gr. B and Alloy 152, the resistances on corrosion and stress corrosion crack growth were decreased, and the hardness was increased.

Next, at further step, the number of precipitates was decreased, resulting in the material re-softening and the recovery of the resistances on corrosion and stress corrosion crack growth.

Acknowledgment

This work was financially supported by the International Collaborative Energy Technology R&D Program (no. 20168540000030) of the Korea Institute of Energy Technology Evaluation and Planning (KETEP), which is funded by the Ministry of Trade Industry and Energy (MOTIE) and the Nuclear Safety Research Program through the Korea Radiation Safety Foundation (KORSAFe) and the Nuclear Safety and Security Commission (NSSC), Republic of Korea (Grant No. 1403006)

REFERENCES

[1] Choi, K.J., Kim J.J., Lee B.H., Bahn C.B., and Kim J.H., Journal of Nuclear Material, Vol. 441, pp. 493, 2013.

[2] Y. Tomota et al., Stress Corrosion Cracking Behavior at Inconel and Low Alloy Steel Weld Interfaces", Metallurgical and Materials Transactions A, Vol. 45A pp. 6103, 2014

[3] O.A. Ojo, and M.C. Chaturvedi, Liquation Microfissuring in the Weld Heat-Affected Zone of an Overaged Precipitation-Hardened Nickel-Base Superalloy, Metallurgical and Materials Transactions A, Vol. 38, pp. 356, 2007

[4] P.L. Andresen, and M.M. Morra, Stress Corrosion Cracking of Stainless Steels and Nickel Alloys in High-Temperature Water, Corrosion Vol. 64, pp. 15, 2008

[5] D. Kirkwood, Precipitate number density in a Ni-Al alloy at early stages of ageing, Acta Metallurgica et Materialia Vol. 18, pp. 563, 1970